

CATASTROPHIC BEHAVIOR OF MULTIPLE CORONAL FLUX ROPE SYSTEM

J.Y. DING and Y.Q. HU

*School of Earth and Space Sciences, University of Science and Technology of China, Hefei,
Anhui 230026, People's Republic of China
(e-mail: jyding@mail.ustc.edu.cn)*

and

J.X. WANG

*National Astronomical Observatories, Chinese Academy of Sciences, Beijing 100012,
People's Republic of China*

(Received 15 October 2005; accepted 10 January 2006)

Abstract. A major solar active event called Bastille Day Event occurred in AR 9077 on July 14, 2000. Simultaneous occurrence of a filament eruption, a flare and a coronal mass ejection was observed in this event. Previous analyses of this event show that before the event, there existed an activation and eruption of a huge trans-equatorial filament, which might play a crucial role in triggering the Bastille Day event. This implies that independent flux systems are closely related to and affect each other, which has encouraged us to investigate the catastrophic behavior of a multiple coronal flux rope system with the use of a 2.5-D time-dependent MHD model. A force-free field that contains three separate coronal flux ropes is taken to be the initial state. Starting from this state, we increase either the annular or the axial flux of a certain flux rope to examine the catastrophic behavior of the system in two regimes, the ideal MHD regime and the resistive MHD regime. It is found that a catastrophe occurs if the flux exceeds a certain critical value, or the magnetic energy of the system exceeds a certain threshold: the rope of interest breaks away from the base and escapes to infinity, leaving a current sheet below. Moreover, the destiny of the remainder flux ropes relies on whether reconnection takes place across the current sheet. In the ideal MHD regime, *i.e.*, in the absence of reconnection, these ropes remain to be attached to the base in equilibrium, whereas in the resistive MHD regime they abruptly erupt upward during reconnection and escape to infinity. Reconnection causes the field lines to close back to the base and thus changes the background field outside the attached flux ropes in such a way that the constraint on these ropes is substantially relaxed and the corresponding catastrophic energy threshold is reduced accordingly, leading to a catastrophic eruption of these ropes. Since magnetic reconnection is generally inevitable when a current sheet forms and develops through an eruption of one flux rope, the eruption of this flux rope must lead to an eruption of the others. This provides an example to demonstrate the interaction between several independent magnetic flux systems in different regions, as implied by the Bastille Day event, and may serve as a possible mechanism for sympathetic events occurring on the Sun.

1. Introduction

While various models have been developed to explain coronal mass ejections (CMEs) in the literature (Forbes and Isenberg, 1991; Wolfson and Low, 1992; Mikic and Linker, 1994; Forbes and Priest, 1995; Lin *et al.*, 1998; Antiochos,

DeVore, and Klimchuk, 1999; Amari *et al.*, 2000), a good deal of attention has been paid to coronal magnetic flux rope models (see reviews by Forbes (2000), Low (2001), and Hu (2005)). Recently, 2.5-D MHD simulations in spherical coordinates were carried out to study the catastrophic behavior of a flux rope system. A common conclusion was reached saying that the system exhibits a catastrophic behavior for various types of background fields, a bipolar (fully closed or partly opened) (Hu, Li, and Xing, 2003; Li and Hu, 2003), a quadrupolar (Zhang, Hu, and Wang, 2005), or an octapolar field (Ding and Hu, 2005; Peng and Hu, 2005), and in the presence of a background solar wind as well (Sun and Hu, 2005). Moreover, a magnetic energy threshold was identified in these studies in such a way that a catastrophe occurs as the threshold is exceeded. For bipolar background field cases, Li and Hu (2003) found a threshold that is larger than the corresponding open field energy by about 8%. The same percentage was acquired by Sun and Hu (2005) when a solar wind coexists with the flux rope system. It seems that the threshold is nearly independent of the detailed properties of the flux rope properties and background field configurations. However, if a topologically more complicated field such as an octapole field is taken as the background, the catastrophic energy threshold was found to clearly depend on both the properties of the flux rope and the configurations of the background field, as demonstrated by Peng and Hu (2005) and Ding and Hu (2005). Not only the energy threshold varies, but also the catastrophic behavior changes for a background field of complex topology. For instance, a quadrupolar field with a neutral point in the corona was used by Zhang, Hu, and Wang (2005) to show that a double catastrophe occurs for a flux rope system, and after catastrophe the flux rope levitates in the corona in equilibrium rather than escapes to infinity. In a word, the flux rope system has a more complicated catastrophic behavior if the background field is a multipolar one.

To our knowledge, only a single flux rope is considered in previous studies of catastrophe. What will the consequence be if the system contains more flux ropes then? And, is there any influence of the eruption of one flux rope because of catastrophe on the status of the others? To answer these questions is quite interesting in their own right, and may inspire us as well in seeking for physical mechanisms for the so-called sympathetic events defined as two successive events in different active regions with one caused by another. Observational evidence has been found in terms of temporal overlap of the events and physical connection between relevant active regions for both sympathetic flares (Gopalswamy *et al.*, 1999; Zhang *et al.*, 2000; Bagala *et al.*, 2000; Wang *et al.*, 2001) and sympathetic CMEs (Moon *et al.*, 2003; Chen *et al.*, 2005). The well-known Bastille Day event on July 14 2000 serves as a good example. This event is characterized by a simultaneous occurrence of a filament eruption, a flare and an extended Earth-directed coronal mass ejection. Wang *et al.* (2005) argued that it was not a single active region phenomenon, but an event clearly involving interaction between a trans-equatorial filament and the magnetic fields of AR 9077 and 9082. The activation and eruption of the huge trans-equatorial filament preceded seems to be the cause of the Bastille Day event.

Besides, Moon *et al.* (2002) found strong statistical evidence for the existence of sympathetic flares. Nevertheless, while it is widely believed that sympathetic events do exist on the Sun, the real mechanism has not been well understood. Many suggestions were made on possible triggering agents for sympathetic events in each of the references cited above, such as energetic particles, shock waves, heat conduction, fast and slow-mode waves, Alfvén waves, subphotospheric sources, and so on. Nevertheless, they remain at a qualitative level in varying degrees and can hardly offer tenable arguments. Therefore, one major target of this study is to propose an alternative new model for sympathetic events on the Sun by examining the catastrophic behavior of a multiple flux rope system.

We start with a force-free field that contains three bipolar fields: A central one across the equator and a bipolar field on each side. A flux rope is present within each bipolar field, and each flux rope is characterized by its annular and axial fluxes. By adjusting the two fluxes of each flux rope separately, we examine the catastrophic behavior of the whole system in both ideal and resistive MHD regimes. The emphasis is placed on the interaction among the three flux ropes. The basic equations and the initial conditions are described in Section 2, the catastrophic behavior of the multiple flux rope system is discussed in Section 3, and we conclude our work in Section 4.

2. Basic Equations and Initial Conditions

For 2.5-D MHD problems in spherical coordinates (r, θ, φ) , one may introduce a magnetic flux function $\psi(t, r, \theta)$ to express the magnetic field by

$$\mathbf{B} = \nabla \times \left(\frac{\psi}{r \sin \theta} \hat{\varphi} \right) + \mathbf{B}_\varphi, \quad \mathbf{B}_\varphi = B_\varphi \hat{\varphi}, \quad (1)$$

where B_φ is the azimuthal component of the magnetic field. The 2.5-D resistive MHD equations are cast in the following form

$$\frac{\partial \rho}{\partial t} + \nabla \cdot (\rho \mathbf{v}) = 0, \quad (2)$$

$$\begin{aligned} \frac{\partial \mathbf{v}}{\partial t} + \mathbf{v} \cdot \nabla \mathbf{v} + \frac{1}{\rho} \nabla p + \frac{1}{\mu \rho} [L\psi \nabla \psi + \mathbf{B}_\varphi \times (\nabla \times \mathbf{B}_\varphi)] \\ + \frac{1}{\mu \rho r \sin \theta} \nabla \psi \cdot (\nabla \times \mathbf{B}_\varphi) \hat{\varphi} + \frac{GM_\odot}{r^2} \hat{r} = 0, \end{aligned} \quad (3)$$

$$\frac{\partial \psi}{\partial t} + \mathbf{v} \cdot \nabla \psi - \frac{1}{\mu} \eta r^2 \sin^2 \theta L\psi = 0, \quad (4)$$

$$\begin{aligned} \frac{\partial B_\varphi}{\partial t} + r \sin \theta \nabla \cdot \left(\frac{B_\varphi \mathbf{v}}{r \sin \theta} \right) + \left[\nabla \psi \times \nabla \left(\frac{v_\varphi}{r \sin \theta} \right) \right]_\varphi \\ - \frac{1}{\mu r \sin \theta} \nabla \eta \cdot \nabla (r \sin \theta B_\varphi) - \frac{1}{\mu} \eta r \sin \theta L (r \sin \theta B_\varphi) = 0, \end{aligned} \quad (5)$$

$$\frac{\partial T}{\partial t} + \mathbf{v} \cdot \nabla T + (\gamma - 1) T \nabla \cdot \mathbf{v} - \frac{(\gamma - 1)}{\rho R} \eta \mathbf{j}^2 = 0, \quad (6)$$

where

$$L \equiv \frac{1}{r^2 \sin^2 \theta} \left(\frac{\partial^2}{\partial r^2} + \frac{1}{r^2} \frac{\partial^2}{\partial \theta^2} - \frac{\cot \theta}{r^2} \frac{\partial}{\partial \theta} \right), \quad (7)$$

$$\mathbf{j} = \frac{1}{\mu} \nabla \times \mathbf{B} = -\frac{1}{\mu} r \sin \theta L \psi \hat{\phi} + \frac{1}{\mu} \nabla \times (B_\varphi \hat{\phi}), \quad (8)$$

ρ is the density, \mathbf{v} is the flow velocity, T is the temperature, $p = \rho RT$ is the gas pressure, R is the gas constant, μ is the vacuum magnetic permeability, G is the gravitational constant, M_\odot is the mass of the Sun, η is the resistivity, and $\gamma (= 1.05)$ is the polytropic index. The ideal MHD version of these equations is obtained by taking $\eta = 0$.

A symmetry is assumed relative to the equator, and the computational domain is taken to be $1 \leq r \leq 30$ in the unit of R_\odot (R_\odot is the solar radius) and $0 \leq \theta \leq \pi/2$, discretized into 130×90 grid points. The grid spacing increases according to a geometrical series of common ratio 1.03 from 0.02 at the base ($r = 1$) to 0.86 at the top ($r = 30$), whereas a uniform mesh is adopted in the θ -direction. The multistep implicit scheme (Hu, 1989) is used to solve Equations (2)–(6). The boundary conditions are the same as described in Ding and Hu (2005).

The initial corona is in isothermal static equilibrium with a temperature $T = T_0 = 2 \times 10^6$ K and a density $\rho = \rho_0 = 1.67 \times 10^{-13}$ kg m $^{-3}$ at the coronal base, where T_0 and ρ_0 are taken to be the units for temperature and density, respectively. As far as the initial magnetic field is concerned, two versions of force-free fields are used in this study; each of them contains three isolated coronal flux ropes, as shown in Figure 1c and d, respectively. These force-free fields are obtained in the way described below.

First of all, we choose a potential field produced by an octapole, of which the normalized magnetic flux function is given by

$$\psi(r, \theta) = \frac{(3 + 5 \cos 2\theta) \sin^2 \theta}{2r^3}, \quad (9)$$

where r is in the unit of R_\odot and ψ is in the unit of a certain constant ψ_0 . Some other units are $B_0 = \psi_0 / R_\odot^2$ for magnetic field strength, $E_0 = 4\pi B_0^2 R_\odot^3 / \mu$ for energy, $v_A = B_0 / \sqrt{\mu \rho_0}$ for velocity, and $\tau_A = R_\odot / v_A$ for time. In this study we take 0.01

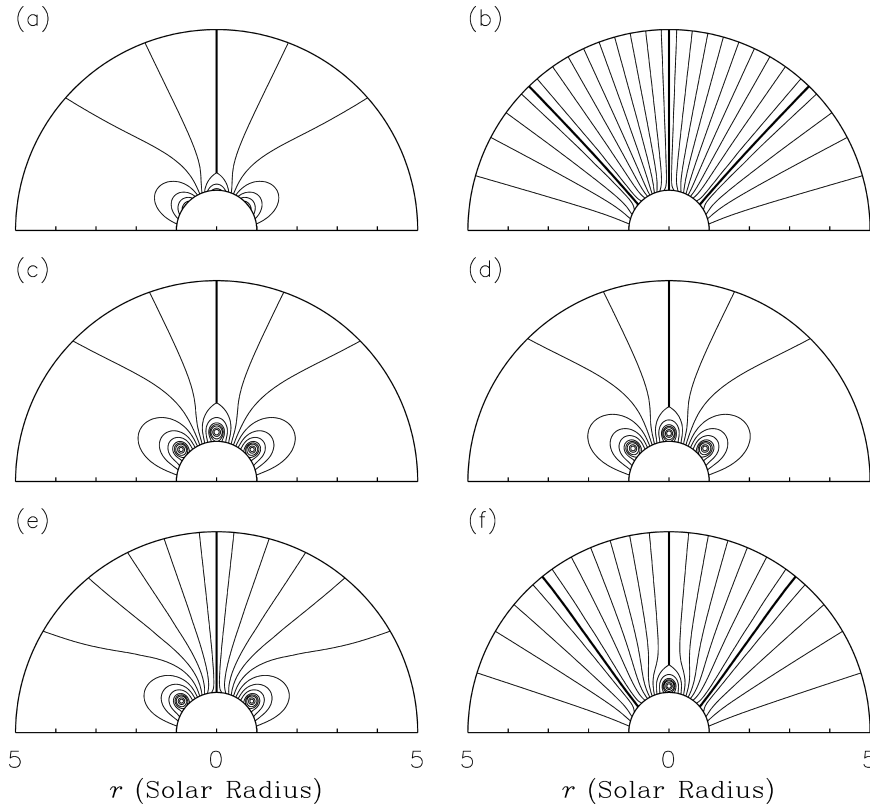


Figure 1. Magnetic configurations for (a) the partly-open octapole field with $\psi = \psi_N = 0.5$, (b) the fully-open octapole field, (c) state A, (d) state B, (e) the corresponding partly-open field of state A, and (f) the corresponding partly-open field of state B. The *thick solid curves* represent the current sheets. Note that states A and B have similar configurations and differ from each other only slightly in the fluxes of the ropes as listed in Table I.

for $\beta = 2\mu\rho_0 RT_0/B_0^2$, the characteristic ratio of gas pressure to magnetic pressure, resulting in $B_0 = 1.18 \times 10^{-3}$ T, $\psi_0 = 5.72 \times 10^{14}$ Wb, $E_0 = 4.69 \times 10^{27}$ J, $v_A = 2570$ km s $^{-1}$, and $\tau_A = 271$ s. As pointed out by Ding and Hu (2005), the octapole field consists of three bipolar fields, centered at $\theta = \theta_c$, $\pi/2$, $\pi - \theta_c = (\theta_c = 43.6^\circ)$, respectively. At the base, ψ takes a maximum of 1 at the equator ($\theta = \pi/2$) and a minimum of -0.8 at $\theta = \theta_c$, and vanishes at the pole ($\theta = 0$).

The following two steps in constructing the two initial fields shown in Figure 1c and d are implemented by the relaxation method proposed by Hu (2004) and used by Ding and Hu (2005) based on the ideal MHD version of Equations (2)–(6). In terms of this method, the temperature and density are reset to their initial values at each time step in order to strictly achieve the force-free condition, and our intention is to obtain a force-free field solution rather than to examine the temporal evolution of the system. In the first step, we change the central bipolar field from completely

closed to partly opened, and the result is shown in Figure 1a, where a thick solid curve denotes the equatorial current sheet, at which $\psi = \psi_N = 0.5$. Parenthetically, if the three bipolar fields are all open, we obtain a fully-open field shown in Figure 1b. In the second step, a flux rope is introduced within each bipolar field, resulting in a force-free field containing three isolated flux ropes. Each rope is characterized by its annual magnetic flux per radian and axial magnetic flux, denoted by Φ_{pc} and $\Phi_{\varphi c}$ for the central flux rope across the equator, and Φ_{pf} and $\Phi_{\varphi f}$ for each of the two flux ropes in the flank. Tentative calculations show that the system exhibits a catastrophic behavior with respect to each of the four fluxes, *i.e.*, a catastrophe occurs as one of the fluxes exceeds a certain critical value for a given set of the other three fluxes, resulting in an eruption of the related flux rope. We may keep either Φ_{pf} and $\Phi_{\varphi f}$ or Φ_{pc} and $\Phi_{\varphi c}$ invariant, and increase the two remainder fluxes gradually so as to eventually locate the catastrophic point. For instance, when we fix $\Phi_{pf} = 0.69$ and $\Phi_{\varphi f} = 0.17$, a catastrophe is about to occur when $\Phi_{pc} = 0.79$ and $\Phi_{\varphi c} = 0.13$. The system is in a metastable equilibrium at this point, and its magnetic configuration is shown in Figure 1c; a further slight increase of either Φ_{pc} or $\Phi_{\varphi c}$ leads to a catastrophe of the system, in which the central flux rope erupts upward and escapes to infinity with a fraction of the characteristic Alfvén speed v_A , leaving a vertical current sheet below. The system approaches another force-free field with the central bipolar field fully opened, as shown in Figure 1e. The metastable state shown in Figure 1c is then taken to be one of the initial force-free fields, called state A hereinafter. The field shown in Figure 1e is defined as its corresponding partly-open field. On the other hand, when we fix $\Phi_{pc} = 0.79$ and $\Phi_{\varphi c} = 0.12$, a similar metastable state is found to be located at $\Phi_{pf} = 0.75$ and $\Phi_{\varphi f} = 0.18$, and the magnetic configuration at this point is shown in Figure 1d, labeled B as another initial state. Starting from state B, a slight increase of either Φ_{pf} or $\Phi_{\varphi f}$ leads to a catastrophe of the system, in which the flux ropes in the flank erupt upward and escape to infinity with a fraction of v_A , leaving a longitudinal current sheet below each flux rope. As a result, we obtain a force-free field with the flux ropes in the flank fully opened, as shown in Figure 1f, and it serves as the corresponding partly-open field of state B. For states A and B and their corresponding partly-open fields obtained above, we calculate the magnetic energy E , normalized by E_0 , with the use of (see Ding and Hu, 2005)

$$E = \frac{1}{2} \int_1^{30} dr \int_0^{\pi/2} B^2 r^2 \sin \theta d\theta + \frac{30^3}{2} \int_0^{\pi/2} (B_r^2 - B_\theta^2)_{r=30} \sin \theta d\theta, \quad (10)$$

and the results are 4.13 and 3.77 for state A and its corresponding partly-open field, and 4.20 and 3.55 for state B and its corresponding partly-open field. The catastrophic energy threshold is then 4.13 for state A and 4.20 for state B, which exceed the corresponding partly-open field energy by 10 and 18%, respectively. The excess energy of the metastable state over the related partly-open state, 0.36 and 0.65, amounts to 32 and 57% of the potential field energy (1.14) for state A and B, respectively. Incidentally, using Equation (10), we find $E = 1.23$ for the

TABLE I

Magnetic fluxes of ropes and energy for the fields shown in Figure 1, and ‘-’ means that the corresponding flux rope is absent.

Field in	Φ_{pc}	$\Phi_{\varphi c}$	Φ_{pf}	$\Phi_{\varphi f}$	E	Note
Figure 1a	-	-	-	-	1.23	Partly-open
Figure 1b	-	-	-	-	3.59	Fully-open
Figure 1c	0.79	0.13	0.69	0.17	4.13	State A
Figure 1d	0.79	0.12	0.75	0.18	4.20	State B
Figure 1e	-	-	0.69	0.17	3.77	Partly-open A
Figure 1f	0.79	0.12	-	-	3.55	Partly-open B

partly-open octapole field in Figure 1a, and 3.59 for the corresponding fully-open field in Figure 1b. The magnetic fluxes of the ropes and the magnetic energy of the fields shown in Figure 1 are summarized in Table I.

3. Catastrophic Behavior of the Multiple Flux Rope System

As just mentioned, the multiple flux rope system has a catastrophic behavior as a single flux rope system does. The related flux rope erupts upward when a catastrophe takes place. This conclusion is not surprising, but agrees with our expectations. Our main concern in this study, however, is the response of the remaining flux rope to such an eruption. A trivial result is that they remain to be attached to the coronal base, whereas a more interesting one is their subsequent eruption. The latter may serve as a mechanism for sympathetic events on the Sun. To judge what the result will be, we carry out time-dependent MHD simulations to study the temporal evolution of the whole system after catastrophe, taking states A and B as the initial magnetic fields. During the simulations we do not reset the temperature and density during the simulations as we did in the relaxation method, but let them evolve with time according to MHD equations. The magnetic field is no longer force-free, but evolves in accordance with MHD equations, too. To initiate a catastrophe of the multiple flux rope system, we may increase one of the two fluxes of either the central flux rope starting from state A or the two ropes in the flank starting from state B. The simulations are then carried out in both ideal MHD regime with $\eta = 0$ and resistive MHD regime with $\eta = 0.01$ (in the unit of $\mu v_A R_\odot$) localized in the neighborhood of the newly formed current sheet below the erupting flux rope. Now let us examine what happens under these two situations.

3.1. IDEAL MHD REGIME

For the ideal MHD case with $\eta = 0$, we first take state A shown in Figure 1c as the initial state and increase Φ_{pc} from 0.79 to 0.80 with $\Phi_{\varphi c} = 0.13$ fixed. A catastrophe

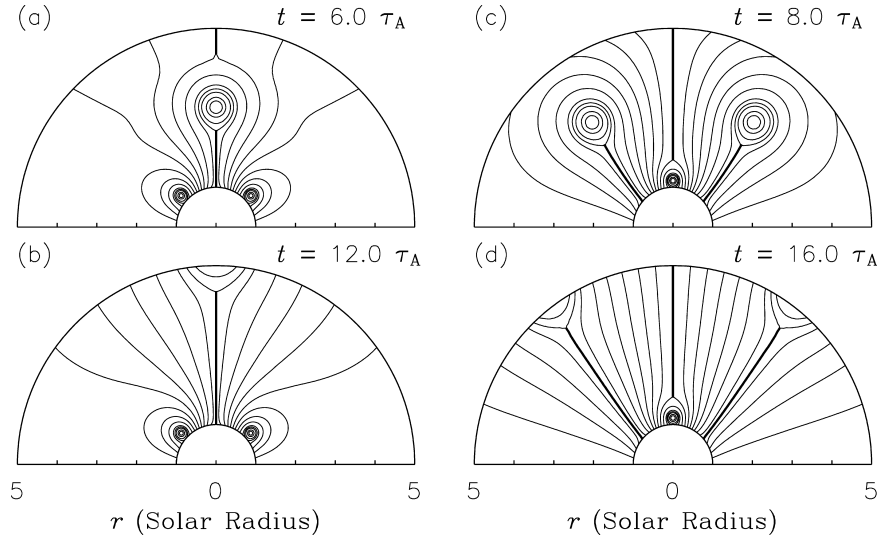


Figure 2. Magnetic configurations at two separate times in the ideal MHD regime for the cases associated with state A (panels a and b) and state B (panels c and d). The *thick solid curves* represent the current sheets.

takes place as shown in Figure 2a and b in terms of the magnetic configurations at two separate times. The central flux rope breaks away from the base and erupts upward in a fraction of the Alfvén speed, whereas the flux ropes in the flank remain to be attached to the base. Similarly, we may increase $\Phi_{\varphi c}$ from 0.13 to 0.14 with $\Phi_{pc} = 0.79$ fixed. A catastrophe also occurs accompanied by an eruption of the central flux rope, and the flux ropes in the flank remain to be attached to the base, too.

Then state B shown in Figure 1d is taken as the initial state instead, and we increase $\Phi_{\varphi f}$ from 0.75 to 0.76 with $\Phi_{\varphi f} = 0.18$ fixed. A catastrophe takes place, as shown in Figure 2c and d in terms of the magnetic configurations at two separate times. The flux ropes in the flank erupt in this case, whereas the central flux rope remains to be attached to the base. Similarly, we may increase $\Phi_{\varphi f}$ from 0.18 to 0.19 with $\Phi_{pf} = 0.75$ fixed. A catastrophe also occurs, accompanied by an eruption of the flux ropes in the flank, and the central flux rope remains to be attached to the base.

In summary, in the ideal MHD regime, a rope eruption in one region does not induce an eruption of the rest in the other regions for the present cases. The resultant background field after catastrophe is still capable of constraining the attached ropes in equilibrium without sympathetic eruption. From the angle of energetics, this result is easily understood. For the case associated with state B, the energy of the resultant partly-open field, shown in Figure 1f, is 3.55 that is below the fully-open field energy of 3.59, so a further opening of the central bipolar field is not

energetically permitted, *i.e.*, the flux ropes over there must remain to be attached to the base. For the case associated with state A, on the other hand, the corresponding partly-open field shown in Figure 1e has an energy of 3.77 that is larger than the fully-open field energy 3.59. However, this energy is still less than the relevant catastrophic energy threshold, so that a follow-up eruption of the flux ropes in the flank is prohibited after the central bipolar field is fully opened up by the erupting flux rope. To demonstrate this argument, we start from the partly-open field shown in Figure 1e and gradually increase either Φ_{pf} or $\Phi_{\phi f}$ of the flux ropes in the flank, until a catastrophic point is met. The corresponding catastrophic energy threshold is thus found to be 4.02 and 3.98, respectively, which are both larger than 3.77. Therefore, even if the system after catastrophe is larger than the fully-open field in energy, the flux ropes in the flank remains to be attached to the base in equilibrium.

3.2. RESISTIVE MHD REGIME

Now let us examine what happens in the resistive MHD regime. In both cases discussed in Section 3.1, a longitudinal current sheet is formed below the erupting flux rope. In the ideal MHD regime, no magnetic reconnection is allowed, and the current sheet keeps extending to infinity. On the other hand, if magnetic reconnection takes place across the newly formed current sheet, the field lines of the related bipolar field will close back to the base rather than extend to infinity, which provides a totally different background field for the remaining flux ropes. We will see that these flux ropes undergo a follow-up catastrophic eruption.

For simplicity, we take a localized resistivity given by

$$l\eta = \begin{cases} 0.01, & -0.5 < \text{sign}(\psi_c)(\psi - \psi_c) < 0 \\ 0, & \text{otherwise} \end{cases} \quad (11)$$

where ψ_c is the value of ψ at the current sheet formed by the first eruption after catastrophe, 1 for state A and -0.8 for state B, and η is the unit of $\mu v_A R_\odot$, $\eta = 0.01$ being equivalent to a Lundquist number of 100. The resistance is limited to the vicinity of the current sheet with a half-width of 0.5 in ψ . Notice that new current sheets will be formed by the second eruption induced by the first, but no resistance is added to them.

The calculations are repeated for the two cases discussed in Section 3.1 but with resistivity given by Equation (11). Figure 3a–c show the magnetic configuration of the solution at three separate times associated with state A, where $t = 6.0\tau_A$ represents the time at which the flux ropes in the flank start to erupt, whereas the central rope is separated from the base and its axis reaches $6.2 R_\odot$ (Figure 3b). Reconnection takes place across the vertical current sheet right below the erupting central rope and causes the field lines to close back to the base. The magnetic energy of the system at this point is found to be 3.42 that is larger than 2.23, the energy of the corresponding partly-open field in which the central bipolar field is completely

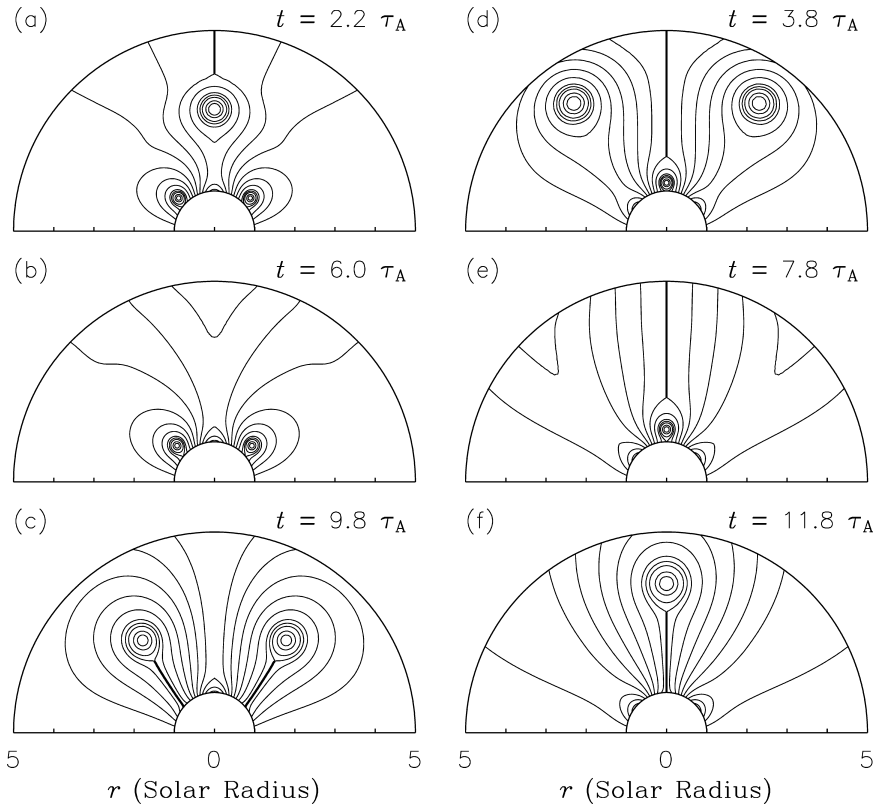


Figure 3. Magnetic configurations at three separate times in the resistive MHD regime for the cases associated with state A (panels a–c) and state B (panels d–f). The *thick solid curves* represent the current sheets.

closed and the bipolar fields in the flank are fully opened. During the eruption of the flux ropes in the flank, a longitudinal current sheet is formed below each rope, but we have not added any resistance over there as mentioned above.

For the case associated with state B, we obtain similar results as shown in Figure 3d–f. Here $t = 7.8\tau_A$ is the time when the central flux rope starts to erupt, whereas the axis of the flux ropes in the flank reaches $6.7 R_\odot$ (Figure 3e). Reconnection takes place across the longitudinal current sheets right below these ropes and causes the field lines to close back to the base. The magnetic energy of the system at this point is found to be 2.84 that is larger than 1.64, the energy of the corresponding partly-open field in which the central bipolar field is fully opened and the bipolar fields in the flank are completely closed. During the eruption of the central flux rope, a vertical current sheet is formed below each rope, but we have not added any resistance over there either.

In summary, the multiple flux rope system exhibits a special catastrophic behavior in the resistive MHD regime: one rope eruption is followed by eruption of

the remainder ropes. Magnetic reconnection causes the field lines to close back to the base, which reduces the constraint of the background field on the attached flux ropes and leads to their eventual eruption. The energy of the system right before the onset of the eruption of the attached flux ropes exceeds that of the corresponding partly-open field and the expected catastrophic energy threshold as well, so their eruption is energetically permitted.

4. Discussions and Conclusions

Based on a 2.5-D time-dependent MHD model, we investigate the catastrophic behavior of a multiple flux rope system containing three flux ropes embedded in three separate arcades. To our knowledge, this is the first MHD simulation, in which more than one flux rope are involved. The system exhibits a catastrophe as a single flux rope system does: any of the flux ropes may erupt independently in a catastrophic manner if its magnetic fluxes exceed certain critical values. A catastrophic energy threshold is also found to exist and exceed the corresponding partly-open field energy. However, our main concern in this study lies in the destiny of the remaining flux ropes after such an eruption. It is shown that the destiny of these ropes depends on whether reconnection takes place across the current sheet formed below the erupting rope. In the ideal MHD regime, *i.e.*, in the absence of reconnection, these ropes remain to be attached to the base in equilibrium, whereas in the resistive MHD regime they abruptly erupt upward during reconnection and escape to infinity. Reconnection causes the field lines to close back to the base and thus changes the background field outside the attached flux ropes in such a way that the constraint on these ropes is substantially relaxed and the corresponding catastrophic energy threshold is reduced accordingly, leading to a catastrophic eruption of these ropes. Since magnetic reconnection is generally inevitable when a current sheet forms and develops through an eruption of one flux rope, the eruption of this flux rope must lead to an eruption of the others. This provides an example to demonstrate the interaction between several independent magnetic flux systems in different regions, as implied by the Bastille Day event, and may serve as a possible mechanism for sympathetic events occurring on the Sun.

For the present multiple flux rope model, the triggering agent for the interaction between different bipolar field regions is the magnetic connection and interaction among them. Different flux ropes share the same large-scale background field, and in fact, they construct a specific background for each other. When one flux rope erupts followed by magnetic reconnection, the background field changes substantially for the remaining flux ropes. This favors a follow-up catastrophic eruption of these ropes. During this process, magnetic reconnection plays a crucial role in relaxing the constraint and reducing the catastrophic energy threshold for the remainder flux ropes that would be attached to the solar surface otherwise. Therefore, a full

exploration of the large-scale field structures among different active regions is necessary in diagnosing sympathetic events on the Sun, especially for sympathetic CMEs (see Zhou *et al.*, 2005).

Acknowledgements

The work was supported by the National Natural Science Foundation of China (40274049, 10233050) and the National Key Basic Science Foundation (TG2000078404).

References

- Amari, T., Luciani, J.F., Mikic, Z., and Linker, J.: 2000, *Astrophys. J.* **529**, L49.
- Antiochos, S.K., DeVore, C.R., and Klimchuk, J.A.: 1999, *Astrophys. J.* **510**, 485.
- Bagala, L.G., Mandrini, C.H., Rovira, M.G., and Demoulin, P.: 2000, *Astron. Astrophys.* **363**, 779.
- Cheng, J.X., Fang, C., Chen, P.F., and Ding, M.D.: 2005, *Chinese J. Astron. Astrophys.* **5**, 265.
- Ding, J.Y. and Hu, Y.Q.: 2006, *Solar Phys.* **233**, 45.
- Forbes, T.G.: 2000, *J. Geophys. Res.* **105**, 23, 153.
- Forbes, T.G. and Insensberg, P.A.: 1991, *Astrophys. J.* **373**, 294.
- Forbes, T.G. and Priest, E.R.: 1995, *Astrophys. J.* **446**, 377.
- Gopalswamy, N. *et al.*: 1999, *Astron. Astrophys.* **347**, 864.
- Hu, Y.Q.: 1989, *J. Comput. Phys.* **84**, 441.
- Hu, Y.Q.: 2004, *Astrophys. J.* **607**, 1032.
- Hu, Y.Q.: 2005, in K.P. Dere, J. Wang, and Y. Yan (eds.), *Coronal and Stellar Mass Ejections, IAU Symp.*, **226**, 263.
- Hu, Y.Q., Li, G.Q., and Xing, X.Y.: 2003, *J. Geophys. Res.* **108**, 1072.
- Li, G.Q. and Hu, Y.Q.: 2003, *Chinese J. Astron. Astrophys.* **3**, 555.
- Lin, J., Forbes, T.G., Insensberg, P.A., and Demoulin, P.: 1998, *Astrophys. J.* **504**, 1006.
- Low, B.C.: 2001, *J. Geophys. Res.* **106**, 25, 141.
- Mikic, Z. and Linker, J.A.: 1994, *Astrophys. J.* **430**, 898.
- Moon, Y.-J. *et al.*: 2002, *Astrophys. J.* **574**, 434.
- Moon, Y.-J. *et al.*: 2003, *Astrophys. J.* **588**, 1176.
- Peng, Z. and Hu, Y.Q.: 2005, *Chinese J. Space Sci.* **25**, 81.
- Sun, S.J. and Hu, Y.Q.: 2005, *J. Geophys. Res.* **110**, A05102, doi:10.1029/2004JA010905.
- Wang, H. *et al.*: 2001, *Astrophys. J.* **559**, 1171.
- Wang, J.X. *et al.*: 2005, in K.P. Dere, J. Wang, and Y. Yan (eds.), *Coronal and Stellar Mass Ejections, IAU Symp.*, **226**, 135.
- Wolfson, R. and Low, B.C.: 1992, *Astrophys. J.* **391**, 353.
- Zhang, Y.Z., Hu, Y.Q., and Wang, J.X.: 2005, *Astrophys. J.* **626**, 1096.
- Zhang, C.X., Wang, H.N., Wang, J.X., and Yan, Y.H.: 2000, *Solar Phys.* **195**, 135.
- Zhou, G.P., Wang, J.X., and Zhang, J.: 2005, in K.P. Dere, J. Wang, and Y. Yan (eds.), *Coronal and Stellar Mass Ejections, IAU Symp.*, **226**, 200.